Korean J. Chem. Eng., 37(3), 525-535 (2020)
DOI: 10.1007/s11814-019-0454-0

pISSN: 0256-1115
eISSN: 1975-7220

Nitrogen removal and nitrogenous intermediate production of the heterotrophic membrane-aerated biofilm: A mathematical modeling investigation

Mei Li*, Chunyu Du,***,****, Meichao Lan**,***,****, Zhiye Sun**,***,****, Rukang Liu**,***,****, and Baoan Li**,***,****,†**

*College of Fisheries, Henan Normal University, Xinxiang 453007, P. R. China
**Chemical Engineering Research Center, School of Chemical Engineering and Technology, Tianjin University, Tianjin 300350, P. R. China
***State Key Laboratory of Chemical Engineering, Tianjin University, Tianjin 300350, P. R. China
****Tianjin Key Laboratory of Membrane Science and Desalination Technology, Tianjin University, Tianjin 300350, P. R. China
(*Received 7 October 2019 • accepted 4 December 2019*)

Abstract−A one-dimensional biofilm model was applied to illustrate the nitrogen conversion and removal within the heterogeneous biofilm attached on the gas-permeable membrane with different oxygen transfer coefficients: 7.5 m/d, 1.5 m/d and 0.3 m/d. Integrating the ammonia-oxidizing bacteria-mediating hydroxylamine oxidization pathway during the autotrophic nitrification and the four-step denitrification pathway during the heterotrophic denitrification, the effects of the intra-membrane aeration pressure and the influent COD/N ratio were further quantitatively evaluated on the systematic performance of nitrogen conversion. Dynamic profiles of key nitrogenous intermediates were investigated to further analyze the treatment efficacy of the targeted biofilm system. It is inapplicable for membrane with oxygen transfer coefficient of 0.3 m/d to sustain the biofilm due to the inferior treatment performance under higher influent organics and distinct nitrous oxide (N_2O) production with elevated aeration pressures under lower influent organics. For the oxygen transfer coefficients of 7.5 m/d and 1.5 m/d, N_2O production was detectable for the insufficient carbon source, indicating the significance of hydroxylamine oxidization. Short-cut nitrogen removal pathway could be feasible within the latter biofilm due to the nitrite accumulation, further reduced by supplementing the carbon source. Heterotrophic denitrification would contribute to the N_2O production. Maintaining the biofilm thickness was conducive to short-cut nitrogen removal by regulating the substrate transfer and the biomass distribution along the biofilm. Besides the total nitrogen removal efficiency, the nitrite accumulation and N_2O production were both decreased with the thickening biofilm. Inside the thinner biofilm, a short-cut pathway via nitrite might be the major pathway for nitrogen removal with distinguished N_2O production, which could be mitigated through supplementing the carbon source.

Keywords: Membrane-aerated Biofilm, Oxygen Transfer Coefficient, Nitrous Oxide, COD/N Ratio, Biofilm Modeling

INTRODUCTION

Counter-diffusion between electron acceptors and donors has been identified inside the membrane-aerated biofilm (MAB), the individual regulation between which promotes the formation of stable redox-stratified structure distinguished from the co-diffusional biofilm [1]. Characterized by the excellent oxygen transfer and utilization efficiency and the nitrifier retention, MAB is more appropriate for the highly-efficient biological nitrogen removal (BNR) through the simultaneous nitrification and denitrification (SND) when compared with the co-diffusional biofilm. Besides it is feasible to achieve short-cut nitrogen removal via nitrite with the biomass activity of nitrite-oxidizing bacteria (NOB) inhibited mainly through microbial competition under certain operational conditions [2].

However, great significance should be attached to the production and consumption of nitrogenous intermediates during the BNR process, which shows severe environmental effects despite the low nitrogen conversion ratio [3]. Nitric oxide (NO) and nitrous oxide (N_2O) are both important atmospheric trace gases, which stably exhibit the direct effects on the ozone in the stratosphere leading to the ozone layer depletion. NO is toxic to a wide range of organisms [4]. Furthermore, N_2O is a more potent greenhouse gas than carbon dioxide and methane [5] with the residence time estimated to be 150 years in the atmosphere [6]. It is reported that N_2O with higher solubility [7] can be detected in large-scale emissions during BNR both at lab-scale reactors and full-scale WWTPs regardless of the large variation of the emission values [8,9] substantially affected by the process configuration and operation [3,7-9]. Generally, chemlithoautotrophic ammonia-oxidizing bacteria (AOB) oxidize ammonia into nitrite via hydroxylamine as the predominant energy-generating process, i.e. it is indispensable to sustain molecular oxygen for the ammonia oxidization to hydroxylamine [10]. According to the nitrogen cycle [11], NO and N_2O could be produced through

†To whom correspondence should be addressed.
E-mail: libaoan@tju.edu.cn
Copyright by The Korean Institute of Chemical Engineers.

the AOB-mediating nitrifier denitrification [4,12-15] and hydroxylamine oxidization [16-18] during the nitrification and the anoxic growth of heterotrophic bacteria (HB) during the incomplete denitrification under sub-optimal growth conditions [11,19,20]. The anaerobic ammonia-oxidizing bacteria (AnAOB) and NOB has been validated to be irrelevant with the production and emission of NO and N_2O [11]. Though the actual formation mechanism of nitrogenous intermediates is still disputed, the nitrifier denitrification pathway under oxygen limitation has been widely identified as a key pathway in many pure and enriched AOB cultures, i.e., the major source of NO and N_2O is associated with the nitrite reduction other than the oxidization of ammonia or hydroxylamine, indicating the complex biochemical reactions and electron transfer processes involved in AOB metabolism [3,7,8,21-23]. Studies also demonstrated that the formation of N_2O is always coupled to that of the toxic NO [24,25], but commonly N_2O is the main intermediate from the NO reduction during the SND with higher yield under low oxygen supply [16] or anaerobic conditions [3]. The metabolic turnover of a nitrifying system is closely related with the environmental conditions. The oxygen profile is the key operational parameter affecting the N_2O emission during the nitrification [7-9]. However, pure culture cultivation conditions are strongly different from those prevailing in natural environments and WWTPs. And nitrite accumulation is the key factor affecting the heterotrophic denitrification [6]. In addition, the influent COD/N ratio [26], the substrate and biomass species, and their interaction with the pH value, temperature and sludge retention time (SRT) would further affect the electron competition and relative kinetic processes of the heterotrophic denitrification, the nitrite accumulation, the end-products, and especially the N_2O production and accumulation.

Dynamic variations of N_2O can be on-line monitored, while limited grab-sampling gives inaccurate estimation under the rapid shifting of operational conditions [8]. To conduct a systematic experimental evaluation would be extremely time-consuming for the biofilm system to be stabilized and be representative under each process condition [27]. Conventionally, the fixed emission factors have been applied to estimate the N_2O emission from the wastewater treatment as recommended by the UN'IPCC and various governments, neglecting the effects of process configuration and operational characteristics under variable environmental conditions [28]. In contrast, mathematical modeling has potentially become a reliable predictive tool for quantifying and evaluating the site-specific N_2O emission [19,28] to interpret and reduce the environmental influence of BNR process in terms with the N_2O production and mitigation based on the relevant mechanism, improving the system design and operation to achieve sustainable nitrogen removal.

The N_2O emission from a single-stage nitritation-ANAMMOX system was identified lower than the two-stage systems [7]. As with the biofilm system, profiles of substrate and microbial distribution were closely related with the N_2O dynamics under diversified process parameters. Sabba et al. [29] reported that more N_2O was produced in the biofilm than the suspending activated sludge system due to the stratified structure. It has been investigated that higher nitrite accumulation could be detected within the co-diffusional biofilm due to the AOB location around the exterior biofilm [30] than the counter-diffusional biofilm for the adjacent region of nitrite production and consumption [31]. Then a significantly lower N_2O generation could be specified within the counter-diffusion biofilm, especially the autotrophic nitrogen removal system, than the co-diffusional biofilm for the treatment of wastewater with high influent ammonia [27,30]. A number of researches have been reported on the nitrifying biofilm and autotrophic MAB [30]. For the commonly constructed BNR process [15], nitrite accumulation is critical to short-cut nitrogen removal for the combination of autotrophic nitrification and heterotrophic denitrification. And even the HB growth on decaying biomass or influent impurities could not be negligible during the autotrophic BNR process [3]. For the MAB system, the oxygen supply is key to the nitrogen conversion, mainly impacted by the membrane oxygen transfer coefficient and intra-membrane aeration pressure. It could be speculated that the aerobic growth of HB would generate the oxygen-limitation, further affecting the nitrite accumulation and the N_2O production. Denitrification is crucial to nitrogen removal, the contributions of which to the N_2O production need to be explicitly investigated [8]. And the biomass activity of HB under the anaerobic growth would further inhibit the nitrogen conversion and removal process through the microbial competition. However, few reports were available to interpret the N_2O production during the SND and the short-cut pathway within the heterotrophic MAB under the influent organics.

In this paper, we emphasize the effects of oxygen supply and influent soluble organics on the nitrogen conversion and removal under the fixed influent ammonia based on the mathematical modeling. The hydroxylamine oxidization pathway during nitrification and HB denitrification were integrated to comprehensively elucidate the dynamics of major nitrogenous intermediates and then the biomass and substrate distribution. Furthermore, effects of biofilm thickness were specified to in-depth explore the changing tendency of nitrogenous substances within the targeted MAB and provide the technical support for the potential application.

METHODOLOGY

1. Model Development

Totally, nine dissolved components, including the readily-degradable organic substance (S_S), oxygen (S_{O2}), ammonia-nitrogen (S_{NH4}), hydroxylamine (S_{NH2OH}), nitrite-nitrogen (S_{NO2}), nitrate-nitrogen (S_{NO3}), nitric oxide (S_{NO}), nitrous oxide (S_{N2O}) and dinitrogen (S_{N2}), were involved in the biofilm system. Five particulate components, including the ammonia-oxidizing bacteria (X_{AOB}), nitrite-oxidizing bacteria (X_{NOB}), heterotrophic bacteria (X_{HB}), slowly-degradable organic substance (X_S) and inert biomass (X_I), were introduced into the model (Table S1). Rate expressions for all the processes are detailed in Table S2. Considering the high aeration performance within the MAB and the nitrifier retention around the gas-permeable membrane surface, the single-pathway model of hydroxylamine oxidization, after elementary comparisons with the AOB denitrification reported by Ni et al. [15] and Mampaey et al. [32], was selected for the ammonia conversion process, including the ammonia oxidization to hydroxylamine, the hydroxylamine oxidization to NO and subsequent NO oxidization to nitrite and then NO reduction to N_2O [9,19,33]. The nitrification process was divided into ammo-

nia oxidation and nitrite oxidation to distinguish the nitrifier activity during the BNR process. The lower ammonia utilization rate of AOB when using NO as electron acceptor instead of oxygen was modified by the anoxic correction factor η_{AOB} during the NO reduction. Besides the aerobic growth, anaerobic growth of facultative HB was represented by the four-step denitrification process, according to the framework of activated sludge model for nitrogen (ASMN), which was composed by the successive growth of anaerobic HB on nitrate, nitrite, NO and N_2O. Dinitrogen was considered as the end-product of the denitrification [20]. NO reduction to N_2O during the hydroxylamine oxidization and anaerobic denitrification was processed in parallel during the BNR. Decay of all the three active biomass, AOB, NOB and HB, included both the endogenous respiration and cell lysis to generate X_S and X_I, as reflected by the first-order kinetic process. Transformation of X_S into S_S was attainable through the instantaneous hydrolysis process to sustain HB growth based on the biomass decay. Stoichiometric matrix for the microbial kinetics is specified in Table S3. As indicated, the model in this paper is similar to that of Ni et al. [33] in the application of modeling the N_2O emission from full-scale wastewater treatment plants with the validity and applicability confirmed. However, the constructed model aims to explore the dynamics of nitrogenous intermediates for the heterogeneous counter-diffusional MAB during the SND process. The hydrolysis processes under aerobic and anaerobic conditions were both considered and yields for the anaerobic growth of HB were modified with the correction factor η_Y for nitrogen oxides utilized as the electron acceptor instead of oxygen according to the ASMN model [20]. This work aimed to investigate effects of HB activity on nitrogen conversion and removal for the treatment of bulk liquid with influent organics. Furthermore, the model was primarily utilized for the heterotrophic MAB system to elucidate the systematic performance, which was different from Ni and Yuan [30], where the AOB denitrification was applied for the autotrophic MAB including AOB, NOB and AnAOB. Key biokinetic and stoichiometric parameters well-established in previous study were adopted from literature and detailed in Table S4. Then the AQUASIM software [34] was utilized to implement the simulation and determine dynamic profiles of the substrate and biomass during the BNR process under given process parameters.

2. Simplification and Assumption

Two successive compartments, the completely-mixed gas compartment and the biofilm compartment, were included in the investigated MAB system, between which was the gas-permeable membrane to directly connect the membrane lumen with the biofilm base. Inside the membrane, air was circulated with the 21% oxygen fraction. Diffusion of the particulate components was excluded from both the pore-water within the biofilm and the bulk liquid with neither the biotic nor the abiotic conversions of all the substrates considered. Hydroxylamine oxidation, chemical conversion of free nitrous acid or hydroxylamine, chemodenitrification or the abiotic/abiological N_2O formation were excluded from the modeled system. According to Debus and Wanner [35], the advective velocity (u_F) was introduced to characterize the biofilm growth with the adjustment coefficient for detachment velocity (c_{de}) defined to stabilize the surface detachment. Furthermore, re-attachment of the detached biomass was neglected during the simulation.

Initial composition of the heterogeneous MAB included the 25% AOB, 30% NOB, and 45% HB, which was formed on the planar gas-permeable membrane with the area of 1 m^2. Biofilm thickness was initially set as 10 μm and the thickness of the diffusive boundary layer was maintained as 100 μm. Porosity of the biofilm thickness was settled as 0.8. None of the dissolved components was present inside the pore-water of the biofilm before the stimulation. External resistance of mass transfer was neglected in the ideal-mixing bulk liquid. Gas exchange with the environment or backmixing of N_2O and N_2 into the membrane lumen was neglected throughout the stimulation. For the biofilm, twenty grid points were selected during each simulation.

3. Simulation Strategy

For the oxygen supply, three membrane oxygen transfer coefficients, 7.5 m/d, 1.5 m/d and 0.3 m/d, respectively, were investigated and nine intra-membrane aeration pressures, 0.10 atm, 0.15 atm, 0.20 atm, 0.25 atm, 0.30 atm, 0.35 atm, 0.40 atm, 0.45 atm and 0.50 atm, respectively.

As with the nitrogenous and carbonous substances in the bulk liquid, influent concentration of ammonia in the bulk liquid was maintained as 15 g N/m^3 throughout all the simulations. The influent concentrations of soluble organics were settled as 5 g COD/m^3, 10 g COD/m^3, 15 g COD/m^3, 20 g COD/m^3, 25 g COD/m^3, 30 g COD/m^3, 35 g COD/m^3, 40 g COD/m^3, 45 g COD/m^3 and 50 g COD/m^3, respectively. The COD/N ratios were calculated as 0.33, 0.67, 1.00, 1.33, 1.67, 2.00, 2.33, 2.67, 3.00 and 3.33, respectively.

Systematic performance of nitrogen conversion and removal was evaluated for the biofilm with the thickness of 400 μm, and the dynamic profiles of substrate and biomass were further determined with microbial competition indicated. The production of nitrogenous intermediates was analyzed for biofilm thicknesses of 200 μm, 400 μm, 600 μm, 800 μm and 1,000 μm, respectively.

4. Sensitivity Analysis

Identifiability and relative significance of key parameters on the nitrogen conversion and removal performance was analyzed by the normalized (non-dimensional) absolute-relative sensitivity function of the built-in algorithm of AQUASIM software [34]. A larger value of sensitivity function indicates the more-accurately identifiable parameters. Certain sensitivity analysis was performed for the typical simulation strategies.

RESULTS AND DISCUSSION

1. Systematic Performance of Nitrogen Conversion and Removal

Combined effects of membrane oxygen transfer coefficient, intra-membrane aeration pressure and the influent COD/N ratio were investigated on the systematic performance of nitrogen conversion and removal for MAB with the thickness of 400 μm. It has been reported that the negligibility of NO reduction into N_2O in comparison with the NO oxidization into nitrite is associated with the differences in oxygen affinity between ammonia monooxygenase (AMO) and terminal oxidase [12]. Being the precursor of N_2O, the NO production is commonly lower, which was consistent with the results in this work. Then the N_2O production was primarily analyzed. As in Fig. 1, dynamic profiles of N_2O production and con-

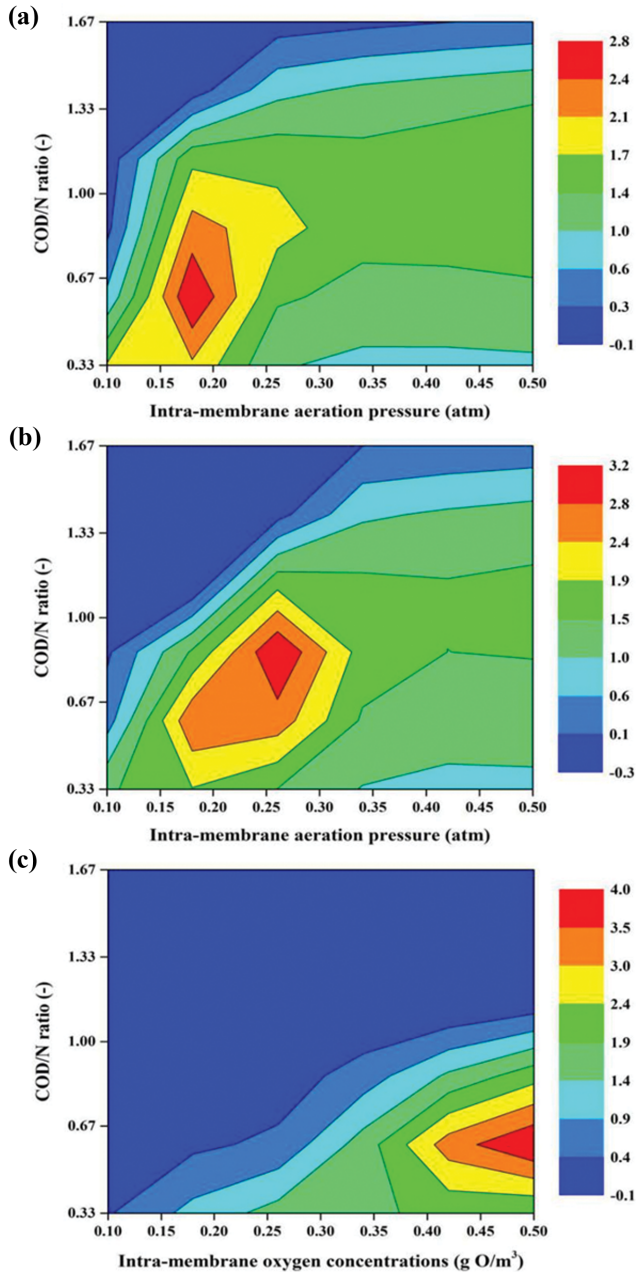


Fig. 1. Effects of intra-membrane aeration pressure and influent COD/N ratio on the dynamic profiles of nitrous oxide production of MAB attached on the membrane with different oxygen transfer coefficients: (a) 7.5 m/d, (b) 1.5 m/d, and (c) 0.3 m/d.

sumption could be regulated through the COD/N ratio or intra-membrane aeration pressure to affect the effective integration of relative components and processes. Distinctively, N_2O production changed differently with the increase of intra-membrane aeration pressure under COD/N ratios of 0.33 to 1.00 among all the three membrane oxygen transfer coefficients.

Removal performance of ammonia and organics could be both improved with the aeration pressure increased. For MAB attached on the membrane with oxygen transfer coefficients of 7.5 m/d and 1.5 m/d, the removal efficiency of total nitrogen exhibited a hump-type changing tendency for the influent COD/N ratio ranging from 0.67 to 1.33. Denitrification was confined for the insufficient conversion of ammonia under lower aeration pressures and the limited carbon source under higher aeration pressures. Hence it is important to increase the aeration pressure for the treatment of higher influent COD/N ratios to sustain the ammonia conversion and complete the denitrification. Significant production of N_2O could be identified for the treatment of influent COD/N ratios of 0.33, 0.67 and 1.00, especially the maximum at COD/N ratio of 0.67 (Fig. 1). In terms of MAB attached on the membranes with oxygen transfer coefficients of 7.5 m/d and 1.5 m/d exhibiting greater removal performance of soluble organics (Fig. S1(b) and Fig. S1(d)), differences in the removal efficiencies between ammonia and total nitrogen indicated that oxygen limitation could be induced by the oxygen consumption of aerobic HB. Then hydroxylamine oxidization was the major pathway for the distinct N_2O production (Fig. 1(a) and Fig. 1(b)). Lowering the aeration pressure, however, should be applied for the MAB attached on membrane with oxygen transfer coefficient of 0.3 m/d (Fig. 1(c)) with removal performance of nitrogen and organics both deteriorated correspondingly (Fig. S1(e) and Fig. S1(f)). And it is indicated that the inhibited growth of aerobic HB promoted the activity of anaerobic HB to perform the denitrification. Furthermore, insufficient oxygen supply suppressed the ammonia oxidization to hydroxylamine and then the limited NO reduction decreased the N_2O production. Subsequently, ammonia conversion and N_2O production were both enhanced with the aeration pressure (Fig. 1(c)). Nitrite accumulation was gradually reduced with the COD/N ratio ranging from 0.33 to 1.33 (data not shown) and the removal performance of total nitrogen was greatly improved, revealing the higher microbial activity of denitrifiers. But the systematic performance of MAB attached on the membrane with oxygen transfer coefficient of 0.3 m/d was remarkably deteriorated, suggesting inferior application potential. Then greater N_2O production was unavoidable, severely restricting the application and generalization.

In addition, for the treatment of lower influent COD/N ratios, similar removal performance could be achieved between those of membrane with oxygen transfer coefficients of 7.5 m/d and 1.5 m/d after improving the aeration pressures. It is observable that increasing the influent COD/N ratio would suppress the ammonia conversion and total nitrogen removal under the aeration pressure from 0.10 atm to 0.25 atm. Removal of organic substances under lower COD/N ratios indicated the significant effects of aerobic HB on ammonia conversion with the microbial activities mediated through further improving the aeration pressures. Then the ammonia conversion was confined by the aeration deficiencies with the influent COD/N ratios increasing, and substantial denitrification further indicated the inhibited ammonia oxidization due to the growth of aerobic HB. The soluble organics were mainly degraded by the aerobic HB under lower COD/N ratios and higher aeration pressures and the removal of total nitrogen was limited by the suppressed ammonia conversion. Consequently, it is essential to maintain sufficient oxygen supply for the treatment of higher influent organics to improve the systematic performance. Then the growth of anaerobic HB would inhibit the aerobic HB and

enhance the ammonia conversion efficiency (Fig. S1(a) and Fig. S1(c)). Significant N_2O production was distinguished under the influent COD/N ratios of 0.33 to 1.33 under the lower aeration pressure (Fig. 1(a) and Fig. 1(b)). Hence it is deduced that the hydroxylamine oxidization could be the main pathway of N_2O production considering the restricted ammonia conversion and insufficient supply of organic substance for denitrification. Besides, the improvement of total nitrogen removal within the two MABs was similar to the aeration pressure increased regardless of the higher ammonia conversion of membrane with oxygen transfer coefficient of 7.5 m/d (Fig. S1(a)) to that of membrane with oxygen transfer coefficient of 1.5 m/d (Fig. S1(c)). Under the aeration pressure of 0.15 atm, nitrite accumulation and N_2O production of membrane with oxygen transfer coefficient of 7.5 m/d (12.12% and 3.22%, respectively) were higher than those of membrane with oxygen transfer coefficient of 1.5 m/d (4.07% and 1.18%, respectively). The total nitrogen removal, however, was similar (22.88% and 23.28%, respectively). Under the aeration pressure of 0.20 atm, nitrite accumulation, N_2O production and total nitrogen removal of membrane with oxygen transfer coefficient of 1.5 m/d (12.72%, 3.32% and 22.80%, respectively) were all higher than those of membrane with oxygen transfer coefficient of 7.5 m/d (10.79%, 2.63% and 15.51%, respectively). The feasibility of short-cut nitrogen removal pathway via nitrite could be recognized. The following sections were targeted on the membrane with oxygen transfer coefficient of 1.5 m/d to specify effects of the intra-membrane aeration pressure and the influent COD/N ratio on nitrogen conversion and removal.

2. Effects of the Intra-membrane Aeration Pressure

Systematic performance of nitrogen conversion and removal was analyzed for the membrane with oxygen transfer coefficient of 1.5 m/d when treating the bulk liquid with the influent COD/N ratio of 0.67.

As indicated in Fig. 2, the ammonia removal efficiency gradually increased and then stabilized with the intra-membrane aeration pressure, while the total nitrogen removal efficiency exhibited a hump-shaped changing tendency. Variation of N_2O production

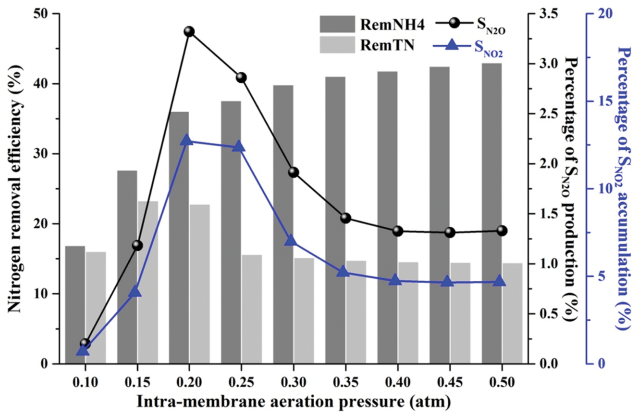


Fig. 2. Dynamics of nitrogen removal, nitrite accumulation and nitrous oxide production with the intra-membrane aeration pressure for MAB on the membrane with oxygen transfer coefficient of 1.5 m/d under influent COD/N ratio of 0.67 (L_F=400 μm).

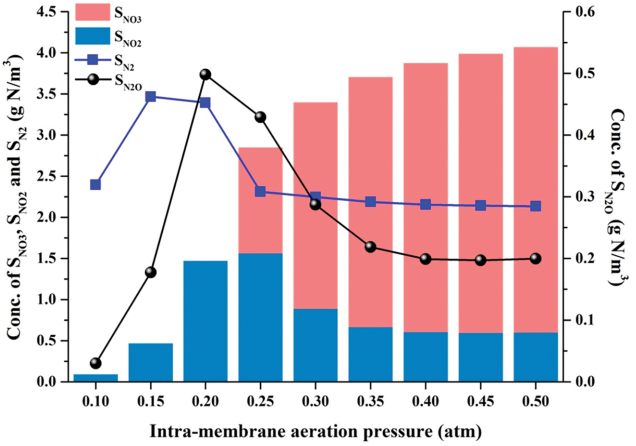


Fig. 3. Variations of nitrogen substances with the intra-membrane aeration pressure for MAB on the membrane with oxygen transfer coefficient of 1.5 m/d under influent COD/N ratio of 0.67 (L_F=400 μm).

was related to that of nitrite accumulation, the maximum of which was achieved under the aeration pressure of 0.20 atm, i.e. 3.32% and 12.72%, respectively. NOB would grow on nitrite as the electron acceptor to further reduce the oxygen consumption for ammonia oxidization to hydroxylamine. Slower rate of nitrite oxidation than the ammonia oxidization causes nitrite accumulation [15]. In addition, denitrification meditated by anaerobic HB could be stimulated by oxygen limitation and nitrite availability [11], which might be associated with suppression of the synthesis and activity of denitrifying enzymes by the oxygen supply, especially the N_2O reductase [8]. Under the intra-membrane aeration pressure of 0.10 atm, lower nitrite could be detected (0.71%) and then the N_2O production (0.20%) for the ammonia oxidization to hydroxylamine confined by the insufficient oxygen supply, which could be improved with the aeration pressure increased. Both AOB and NOB change their metabolic activities significantly at reduced oxygen supply [27], and effects of NOB activity on N_2O production might be related to nitrite consumption. However, the nitrite oxidization to nitrate under higher aeration pressure decreased the nitrite accumulation and N_2O production. The hydroxylamine oxidization was inhibited for increasing the oxygen concentration to sustain the electron competition between oxygen and nitrite under higher oxygen concentration. Hence both the nitrite reduction efficiency and nitrite concentration were further decreased [28]. In particular, the removal efficiency of total nitrogen was greater with certain amounts of nitrite accumulation and remarkable N_2O production under the aeration pressure of 0.20 atm, indicating the feasibility of short-cut nitrogen removal. Although greater ammonia conversion could be identified under higher aeration pressure for the active biomass of aerobic HB suppressed by the insufficient organics, the denitrification conducted by anaerobic HB was further inhibited to consequently decrease the total nitrogen removal. Overall, during the application of targeted MAB for the treatment of bulk liquid with lower COD/N ratios, a short-cut SND pathway could be maintained when lowering the intra-membrane aeration pressure. N_2O production should be promoted due to the nitrite

accumulation for heterotrophic denitrification. And it is critical to supplement the carbon source to eliminate the nitrite remaining in the effluent.

3. Effects of the Influent COD/N Ratio

HB denitrification and reduction of nitrogen oxides are closely coupled with the degradation of soluble organics. For the effect of the influent soluble organics on the systematic performance of nitrogen conversion and removal, the biofilm with the thickness of 400 μm attached on the gas-permeable membrane with the oxygen transfer coefficient of 1.5 m/d was targeted.

In Fig. 4, the ammonia conversion efficiency gradually decreased with the influent COD/N ratio and the total nitrogen removal exhibited the hump-shaped changing tendency. It is evident that the nitrite accumulation was reduced and the influent ammonia was removed as the dinitrogen gas (Fig. 5) with the removal efficiency of total nitrogen mainly affected by the ammonia conversion. Under the intra-membrane aeration pressure of 0.20 atm, growth of aerobic HB was greatly promoted under higher supply of organic substances to compete with the oxygen consumption with AOB and then inhibit the ammonia conversion. However, the nitrite oxidation was greatly suppressed with the nitrite reduction substantially improved. Lower N_2O reduction efficiency resulted in N_2O accumulation and emission. As the important intermediate, higher concentration of nitrite could inhibit the denitrification due to the toxic inhibitory effects and then cause nitrite accumulation [29]. For the influent COD/N ratio of 0.33, higher ammonia conversion could be specified and then the significant nitrite accumulation due to the incomplete heterotrophic denitrification, indicating the N_2O majorly generated from the hydroxylamine oxidization though the accumulation of hydroxylamine and other intermediates, as the NO or NOH under higher ammonia conversion [33]. Removal performance of total nitrogen was slightly improved under the influent COD/N ratio of 0.67 with higher N_2O production (3.32%). The ASMN model [20] was utilized in this work and the competition effects for electron donors among all the four steps during the denitrification were neglected [26]. Denitrifying organisms also increased N_2O and NO production to a lesser extent upon changed concentration profiles of nitrite and dissolved oxygen [3]. The hydroxylamine oxidization and ammonia oxidization were in parallel [19]. The intermediate accumulation under low oxygen and higher nitrite could promote the N_2O production [11]. Higher concentration of nitrite would reverse the nitrite reductase, leading to higher N_2O production. In accordance with the greater ammonia conversion, the HB denitrification might contribute to the N_2O production. It is critical to supplement the soluble organics to avoid the production and accumulation of nitrogenous intermediates, revealing the dependence of total nitrogen removal on ammonia conversion.

Hence it is speculated that a short-cut nitrogen removal pathway could be achieved under the complete ammonia conversion for the application of the targeted MAB to treat the bulk liquid with lower influent COD/N ratios. N_2O production could be distinguished during the HB denitrification under insufficient supply

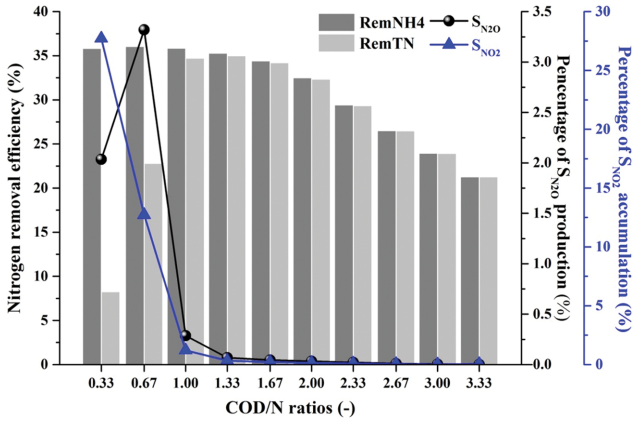


Fig. 4. Dynamics of nitrogen removal, nitrite accumulation and nitrous oxide production with the influent COD/N ratio for MAB on the membrane with oxygen transfer coefficient of 1.5 m/d under intra-membrane aeration pressure of 0.20 atm (L_F=400 μm).

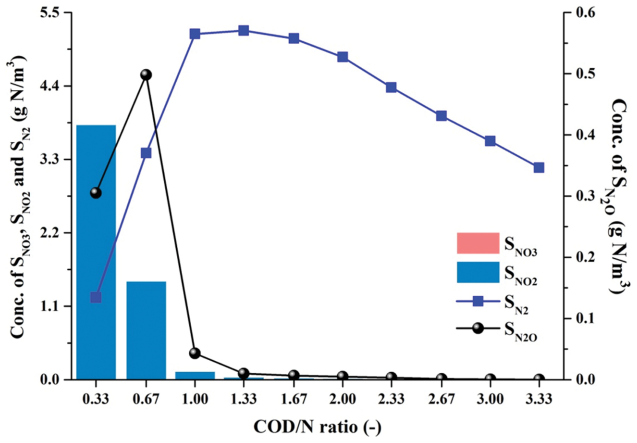


Fig. 5. Variations of nitrogen substances with the influent COD/N ratio for MAB on the membrane with oxygen transfer coefficient of 1.5 m/d under intra-membrane aeration pressure of 0.20 atm (L_F=400 μm).

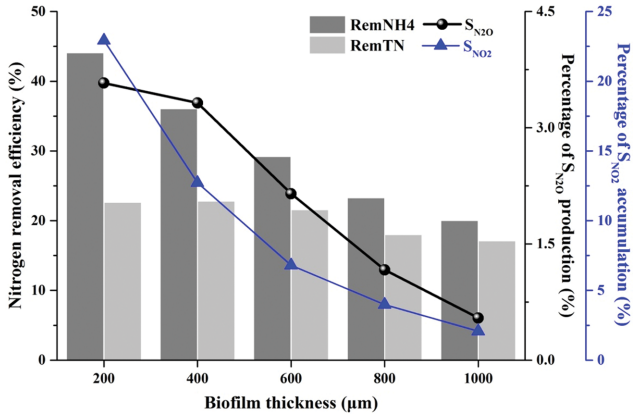


Fig. 6. Effects of biofilm thickness on the nitrogen removal, nitrite accumulation and nitrous oxide production for MAB on the membrane with oxygen transfer coefficient of 1.5 m/d under influent COD/N ratio of 0.67 and intra-membrane aeration pressure of 0.20 atm.

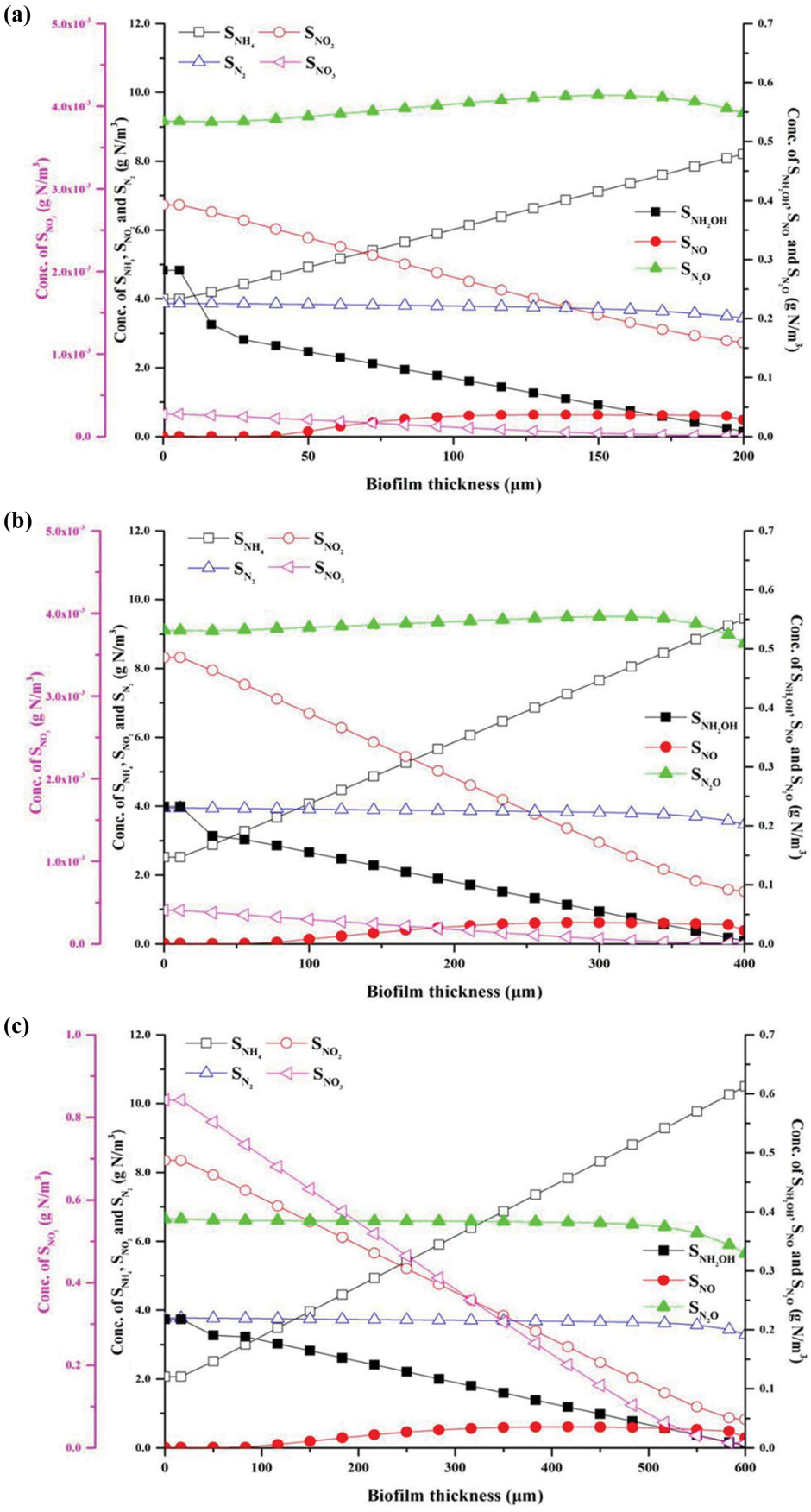


Fig. 7. Concentration profile of nitrogen substances along the biofilm: (a) 200 μm, (b) 400 μm, (c) 600 μm, (d) 800 μm and (e) 1,000 μm.

of soluble organics. Higher COD/N ratios, or the availability of readily degradable organic matter in the influent, would be conducive to inhibiting the N_2O production, i.e. the supplement of carbon source for the HB denitrification to further reduce the nitrite accumulation.

4. Effects of the Biofilm Thickness

The relation of systematic performance of nitrogen conversion and removal with the biofilm thickness was investigated for the biofilm attached on the gas-permeable membrane with the oxygen transfer coefficient of 1.5 m/d under the intra-membrane aeration pressure of 0.20 atm and the influent COD/N of 0.67.

For the low influent COD/N ratios, N_2O was the major intermediate rather than NO (Data unshown). As indicated in Fig. 6, the ammonia conversion deteriorated significantly for the mass transfer of ammonia limited with the biofilm thickening and then the low substrate availability or concentration in the same range of or below the affinity values [15]. Inside the MAB, the growth of anaerobic HB could be detected around the exterior region of the biofilm adjacent to the bulk liquid. Hence denitrification was almost unaffected by the mass transfer of soluble organics. The removal of total nitrogen could be stabilized and mainly determined by the ammonia conversion. It has been noticed that higher N_2O was produced in the thicker, rather than the thinner, co-diffusional autotrophic biofilm or in the suspending activated sludge system, which might be associated with the limited oxygen transfer and then the inhibited nitrite oxidization within the thicker biofilm. Changing tendency of total nitrogen removal performance and N_2O production of the counter-diffusional heterotrophic biofilm were distinct from those of the co-diffusional autotrophic biofilm [27,30]. Liu et al. demonstrated that the N_2O accumulation decreased due to the limited mass transfer with the biofilm thickness in the autotrophic MABR system [36]. Lower ammonia concentration and cer-

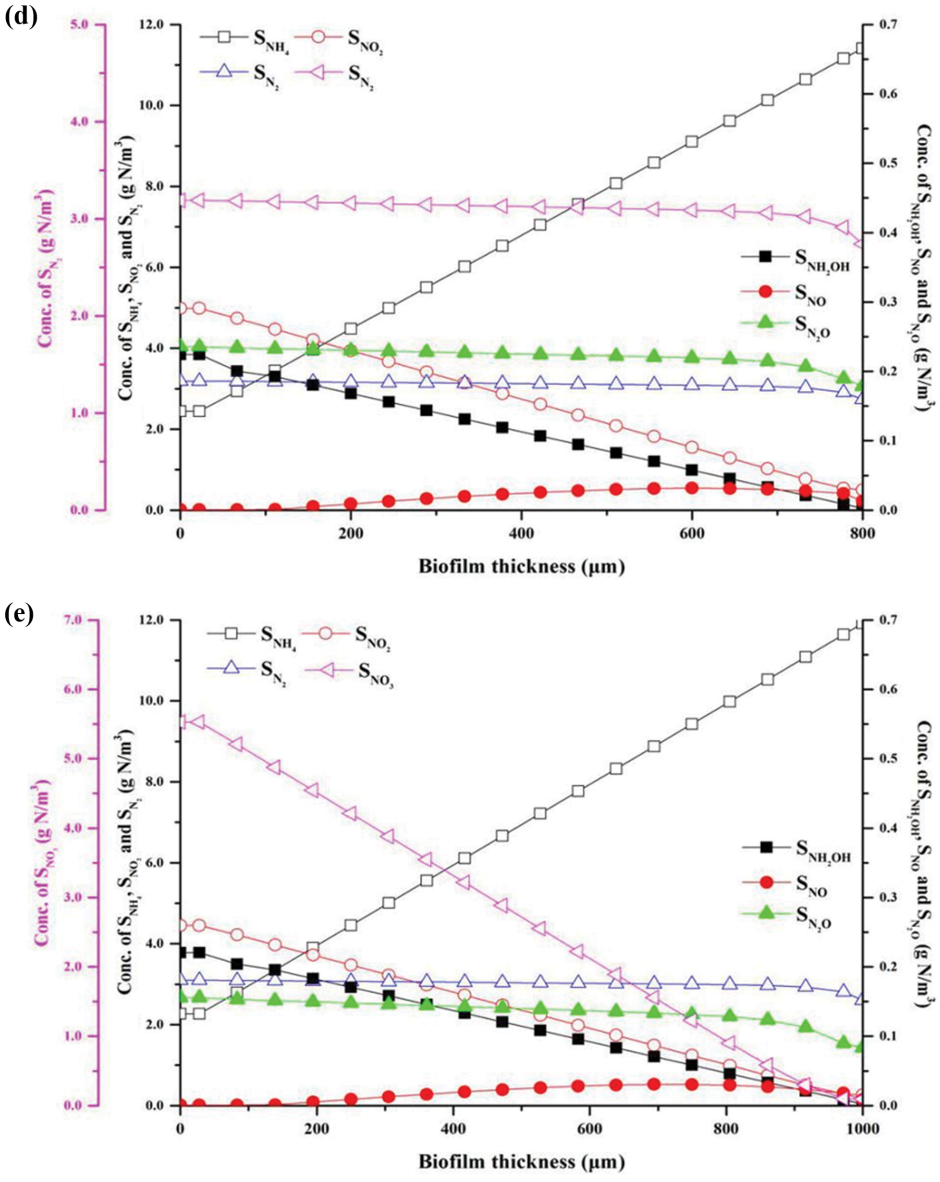


Fig. 7. Continued.

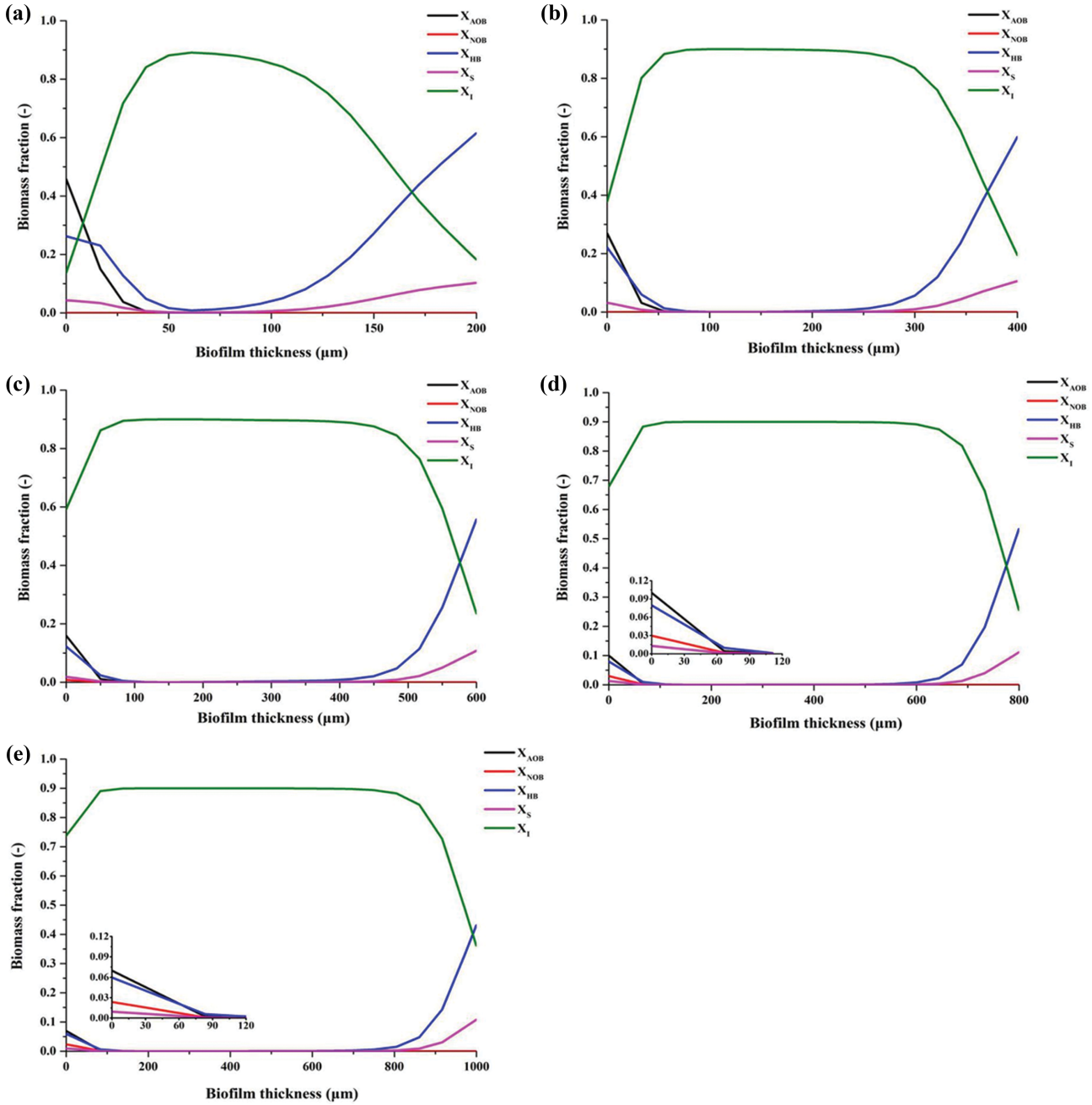


Fig. 8. Profile of biomass fraction along the biofilm: (a) 200 μm, (b) 400 μm, (c) 600 μm, (d) 800 μm and (e) 1,000 μm.

tain oxygen concentrations were conducive to the higher nitrogen removal and lower N_2O production [37]. In this paper, the nitrite accumulation and N_2O production were both decreased with the biofilm thickness. Furthermore, the nitrite oxidization (Fig. 7(c)) was identified and the N_2O production (Fig. 6) was lowered for MAB of 600 μm. The nitrate production was gradually improved (Fig. 7(d) and Fig. 7(e)). Though the reduced availability of ammonia due to the transfer limitation, certain amounts of slow-degradable organics from AOB decay enhanced the growth activity of aerobic HB to further inhibit the ammonia conversion. According to the concentration profile of N_2O along the biofilm (Fig. 7) and the distribution profile of microbial communities within the MAB (Fig. 8), it could be speculated that both the hydroxylamine oxidization and HB denitrification contributed to the N_2O production. For the MABs of 200 μm, 400 μm and 600 μm, it is evident that the nitrite oxidization and the subsequent transfer limitation were both restricted and higher activity of the denitrification region would be identified (Fig. 8(a), Fig. 8(b) and Fig. 8(c)). Consequently, the feasibility of short-cut nitrogen removal via nitrite could be observed. However, with the MAB further thickening to 800 μm (Fig. 8(d)) and 1,000 μm (Fig. 8(e)), the AOB growth was greatly inhibited due to the ammonia limitation, and the NOB activity could be detected to oxidize nitrite into nitrate. Active biomass was significantly reduced with the prolonged SRT. Inside the

biofilm, the activity of aerobic HB was reduced gradually due to the limited transport of soluble organics and insufficient hydrolyzed decayed-biomass with the biofilm thickness. The mass transfer of nitrite and nitrate were both affected by the biofilm thickness to decrease the denitrification activity around the biofilm surface and then the removal of total nitrogen. The regulation of N_2O production would be relevant to the total nitrogen removal [30]. Consequently, the N_2O and N_2 production both decreased (Fig. 7(d) and Fig. 7(e)). Hence the complete denitrification in accordance with the ASMN was the major pathway of nitrogen removal with insignificant N_2O production due to the sufficient supply of organic substances. Above all, the short-cut SND would be the major nitrogen removal pathway within the thinner MAB and more N_2O production originated from the HB denitrification than the hydroxylamine oxidization (3.58% for 200 μm, 3.32% for 400 μm and 2.15% for 600 μm, respectively). Operational parameters would significantly affect the key microbes and then the nitrogen removal pathway [3]. During operation, measures should be taken to regulate the biofilm thickness and further avoid the mass transfer and to particularly control the N_2O production from the thinner MAB performing the short-cut nitrogen removal, e.g. supplementing the carbon source.

5. Sensitivity Analysis

With the built-in algorithms of AQUASIM [34], a sensitivity analysis was conducted to evaluate the model robustness and determine the key parameters on the nitrogen removal performance (i.e., the dissolved nitrogen and nitric oxide concentrations in the effluent) for MAB of 400 μm attached on the membrane with oxygen transfer coefficient of 1.5 m/d under the intra-membrane aeration pressure of 0.20 atm and the influent COD/N ratio of 0.67.

From Fig. S2, the nitrogen removal of MAB was closely associated with the yield coefficient of HB and AOB, indicating the potential competition between nitrite accumulation and consumption and then the NOB affinity for oxygen. N_2O production was closely related to the anaerobic growth of HB on nitrite and NO, suggesting the significance of dynamics of nitrite accumulation and reduction via denitrification as indicated in Fig. S3. Hence, the solid model structure was reliable to predict nitrogen conversion and removal, including the N_2O production and consumption during the short-cut pathway, of the constructed MAB system during the BNR process.

CONCLUSION

A one-dimensional multi-substrate and multi-population biofilm mathematical model was constructed and implemented to illustrate effects of membrane oxygen transfer coefficient, intra-membrane aeration pressure and influent COD/N ratio on the nitrogen conversion and removal and then the production of main nitrogenous intermediates of MAB. It is not applicable for the membrane with inferior aeration characteristics to sustain biofilm while performing the BNR process, especially for the treatment of higher influent COD/N ratios. Though the removal performance could be enhanced under increasing the aeration pressure for the lower influent COD/N ratios, distinct N_2O production was observable. For MABs on the membranes with oxygen transfer coefficients of 7.5 m/d and 1.5 m/d, the N_2O production was detectable for the insufficient carbon source. Both the removal performance of total nitrogen would be greatly improved with the short-cut nitrogen removal pathway feasibly achieved in the latter MAB. Nitrite accumulation, however, promoted N_2O production, and the nitrite in the effluent should be further removed by supplementing the carbon source. Then heterotrophic denitrification would contribute to the N_2O production. Biofilm thickness should be controlled to inhibit the deteriorated nitrogen removal due to the limitation of mass transfer. Inside the thinner heterogeneous MAB, the short-cut SND via nitrite might be the major pathway for nitrogen removal with distinguished N_2O production, which could be mitigated through supplementing the carbon source. The results potentially provide a better understanding of nitrogen conversion and removal and then the intermediate production of counter-diffusional biofilm containing autotrophic nitrifiers and heterotrophic denitrifiers to further improve the design and operation of MAB system for BNR process. Model-based mitigation strategies should be further conducted and validated during the practical application to sustain the validity and applicability.

ACKNOWLEDGEMENT

This work was supported by the National Natural Science Foundation of China [grant numbers: 51478304].

DISCLOSURES

The authors declare no competing financial interest.

SUPPORTING INFORMATION

Additional information as noted in the text. This information is available via the Internet at http://www.springer.com/chemistry/journal/11814.

REFERENCES

1. R. Nerenberg, *Curr. Opin. Biotechnol.*, **38**, 131 (2016).
2. M. Li, C. Y. Du, J. Liu, X. Quan, M. C. Lan and B. A. Li, *Chem. Eng. J.*, **338**, 680 (2018).
3. M. J. Kampschreur, N. C. G. Tan, R. Kleerebezem, C. Picioreanu, M. S. M. Jetten and M. C. M. van Loosdrecht, *Environ. Sci. Technol.*, **42**, 429 (2007).
4. M. J. Kampschreur, C. Picioreanu, N. C. G. Tan, R. Kleerebezem, M. S. M. Jetten and M. C. M. van Loosdrecht, *Water Environ. Res.*, **79**, 2499 (2007).
5. IPCC, *Climate change 2001: the scientific basis*, Cambridge University Press, Cambridge (2001).
6. W. G. Zumft, *Am. Soc. Microbiol.*, **61**, 533 (1997).
7. M. J. Kampschreur, W. R. L. van der Star, H. A. Wielders, J. W. Mulder, M. S. M. Jetten and M. C. M. van Loosdrecht, *Water Res.*, **42**, 812 (2008).
8. M. J. Kampschreur, H. Temmink, R. Kleerebezem, M. S. M. Jetten and M. C. M. van Loosdrecht, *Water Res.*, **43**, 4093 (2009).
9. L. Peng, B.-J. Ni, L. Ye and Z. Yuan, *Chem. Eng. J.*, **281**, 661 (2015).

10. A. B. Hooper, T. Vannelli, D. J. Bergmann and D. M. Arciero, *Antonie van Leeuwenhoek*, **71**, 59 (1997).
11. B. B. Colliver and T. Stephenson, *Biotechnol. Adv.*, **18**, 219 (2000).
12. B.-J. Ni, L. Peng, Y. Law, J. Guo and Z. Yuan, *Environ. Sci. Technol.*, **48**, 3916 (2014).
13. R. Yu, M. J. Kampschreur, M. C. M. van Loosdrecht and K. Chandran, *Environ. Sci. Technol.*, **44**, 1313 (2010).
14. S. W. Kim, M. Miyahara, S. Fushinobu, T. Wakagi and H. Shoun, *Bioresour. Technol.*, **101**, 3958 (2010).
15. B.-J. Ni, M. Ruscalleda, C. Pellicer-Nacher and B. F. Smets, *Environ. Sci. Technol.*, **45**, 7768 (2011).
16. M. Poth and D. D. Focht, *Appl. Environ. Microbiol.*, **49**, 1134 (1985).
17. N. Wrage, G. L. Velthof, M. L. van Beusichem and O. Oenema, *Soil Biol. Biochem.*, **33**, 1723 (2001).
18. L. Poughon, C. G. Dussap and J. B. Gros, *Biotechnol. Bioeng.*, **72**, 416 (2000).
19. B.-J. Ni and Z. Yuan, *Water Res.*, **87**, 336 (2015).
20. W. C. Hiatt and C. P. L. Grady, *Water Environ. Res.*, **80**, 2145 (2008).
21. M. D. Butler, Y. Y. Wang, E. Cartmell and T. Stephenson, *Water Res.*, **43**, 1265 (2009).
22. Q. Yang, X. Liu, C. Peng, S. Wang, H. Sun and Y. Peng, *Environ. Sci. Technol.*, **43**, 9400 (2009).
23. J. Foley, D. de Haas, Z. Yuan and P. Lant, *Water Res.*, **44**, 831 (2010).
24. F. Schreiber, B. Loeffler, L. Polerecky, M. M. M. Kuypers and D. de Beer, *ISME J.*, **3**, 1301 (2009).
25. M. J. Kampschreur, R. Poldermans, R. Kleerebezem, W. R. van der Star, R. Haarhuis, W. R. Abma, M. S. M. Jetten and M. C. M. van Loosdrecht, *Water Sci. Technol.*, **60**, 3211 (2009).
26. Y. Pan, B.-J. Ni, H. Lu, K. Chandran, D. Richardson and Z. Yuan, *Water Res.*, **71**, 21 (2015).
27. L. Peng, J. Sun, Y. Liu, X. Dai and B.-J. Ni, *Sci. Rep.*, **6**, 28880 (2016).
28. B.-J. Ni, Z. Yuan and K. Chandran, *Biotechnol. Bioeng.*, **110**, 153 (2013).
29. F. Sabba, C. Picioreanu, J. Pérez and R. Nerenberg, *Environ. Sci. Technol.*, **49**, 1486 (2015).
30. B.-J. Ni and Z. Yuan, *J. Membr. Sci.*, **428**, 163 (2013).
31. R. Wang, A. Terada, S. Lackner, B. F. Smets, M. Henze, S. Xia and J. Zhao, *Water Res.*, **43**, 2699 (2009).
32. K. E. Mampaey, B. Beuckels, M. J. Kampschreur, R. Kleerebezem, M. C. M. van Loosdrecht and E. I. P. Volcke, *Environ. Technol.*, **34**, 1555 (2013).
33. B.-J. Ni, L. Ye, Y. Law, C. Byers and Z. Yuan, *Environ. Sci. Technol.*, **47**, 7795 (2013).
34. P. Reichert, AQUASIM 2.0d User Manual, *Computer program for the identification and simulation of aquatic systems*, Swiss Federal Institute for Environmental Science and Technology (EAWAG), Dubendorf, Switzerland (1998).
35. O. Debus and O. Wanner, *Wat. Sci. Technol.*, **26**, 607 (1992).
36. Y. Liu, L. Peng, H. H. Ngo, W. Guo, D. Wang, Y. Pan, J. Sun and B.-J. Ni, *Environ. Sci. Technol.*, **50**, 9407 (2016).
37. L. Peng, Y. Liu and B.-J. Ni, *Chem. Eng. J.*, **287**, 217 (2016).

Supporting Information

Nitrogen removal and nitrogenous intermediate production of the heterotrophic membrane-aerated biofilm: A mathematical modeling investigation

Mei Li[*], Chunyu Du[,***,****], Meichao Lan[**,***,****], Zhiye Sun[**,***,****], Rukang Liu[**,***,****], and Baoan Li[**,***,****,†]**

*College of Fisheries, Henan Normal University, Xinxiang 453007, P. R. China
**Chemical Engineering Research Center, School of Chemical Engineering and Technology, Tianjin University, Tianjin 300350, P. R. China
***State Key Laboratory of Chemical Engineering, Tianjin University, Tianjin 300350, P. R. China
****Tianjin Key Laboratory of Membrane Science and Desalination Technology, Tianjin University, Tianjin 300350, P. R. China
(*Received 7 October 2019 • accepted 4 December 2019*)

Table S1. Dissolved and particulate components defined in the model

Component	Definition	Unit
S_S	Readily-degradable organic substrate	g COD/m^3
S_{NH4}	Ammonia	g N/m^3
S_{NH2OH}	Hydroxylamine	g N/m^3
S_{NO2}	Nitrite	g N/m^3
S_{NO3}	Nitrate	g N/m^3
S_{NO}	Nitric oxide	g N/m^3
S_{N2O}	Nitrous oxide	g N/m^3
S_{N2}	Nitrogen	g N/m^3
S_{O2}	Oxygen	g O/m^3
X_{AOB}	Ammonium-oxidizing bacteria	g COD/m^3
X_{NOB}	Nitrite-oxidizing bacteria	g COD/m^3
X_{HB}	Heterotrophic bacteria	g COD/m^3
X_S	Slowly-degradable organics	g COD/m^3
X_I	Inert, non-biodegradable organics	g COD/m^3

Table S2. Stoichiometric matrix of the membrane-aerated biofilm

Process	Component													
	S_{O2}	S_S	S_{NH4}	S_{NH2OH}	S_{NO2}	S_{NO3}	S_{NO}	S_{N2O}	S_{N2}	X_S	X_{HB}	X_{AOB}	X_{NOB}	X_I
1	–1.14		–1	1										
2	$-\frac{1.71-Y_{AOB}}{Y_{AOB}}$		$-i_{NBM}$	$-\frac{1}{Y_{AOB}}$			$\frac{1}{Y_{AOB}}$					1		
3	–0.57				1		–1							
4				–1	1		–4	4						
5			$i_{NBM}-i_{NXI}*f_I$							$1-f_I$		–1		f_I
6	$-\frac{1.14-Y_{NOB}}{Y_{NOB}}$		$-i_{NBM}$		$-\frac{1}{Y_{NOB}}$	$\frac{1}{Y_{NOB}}$							1	
7			$i_{NBM}-i_{NXI}*f_I$							$1-f_I$			–1	f_I
8		1								–1				
9	$-\frac{1-Y_{HB}}{Y_{HB}}$	$-\frac{1}{Y_{HB}}$	$-i_{NBM}$								1			
10		$-\frac{1}{\eta_Y\times Y_{HB}}$	$-i_{NBM}$		$\frac{1-\eta_{HB}\times Y_{HB}}{1.14\times\eta_{HB}\times Y_{HB}}$	$-\frac{1-\eta_{HB}\times Y_{HB}}{1.14\times\eta_{HB}\times Y_{HB}}$					1			
11		$-\frac{1}{\eta_Y\times Y_{HB}}$	$-i_{NBM}$		$-\frac{1-\eta_{HB}\times Y_{HB}}{0.57\times\eta_{HB}\times Y_{HB}}$		$\frac{1-\eta_{HB}\times Y_{HB}}{0.57\times\eta_{HB}\times Y_{HB}}$				1			
12		$-\frac{1}{\eta_Y\times Y_{HB}}$	$-i_{NBM}$				$-\frac{1-\eta_{HB}\times Y_{HB}}{0.57\times\eta_{HB}\times Y_{HB}}$	$\frac{1-\eta_{HB}\times Y_{HB}}{0.57\times\eta_{HB}\times Y_{HB}}$			1			
13		$-\frac{1}{\eta_Y\times Y_{HB}}$	$-i_{NBM}$					$-\frac{1-\eta_{HB}\times Y_{HB}}{0.57\times\eta_{HB}\times Y_{HB}}$	$\frac{1-\eta_{HB}\times Y_{HB}}{0.57\times\eta_{HB}\times Y_{HB}}$		1			
14			$i_{NBM}-i_{NXI}*f_I$							$1-f_I$	–1			f_I

Table S3. Kinetic rate expressions of the membrane-aerated biofilm

Process	Kinetic rate expression (g COD/m^3·d)
Ammonium oxidation to NH_2OH by AOB	$\mu_{AOB,\,AMO}\times\frac{S_{O2}}{K_{AOB,\,O2,\,1}+S_{O2}}\times\frac{S_{NH4}}{K_{AOB,\,NH4}+S_{NH4}}\times X_{AOB}$
NH_2OH oxidation to NO by AOB	$\mu_{AOB,\,HAO,\,1}\times\frac{S_{O2}}{K_{AOB,\,O2,\,2}+S_{O2}}\times\frac{S_{NH2OH}}{K_{AOB,\,NH2OH}+S_{NH2OH}}\times X_{AOB}$
NO oxidation to nitrite by AOB	$\mu_{AOB,\,HAO,\,2}\times\frac{S_{O2}}{K_{AOB,\,O2,\,2}+S_{O2}}\times\frac{S_{NO}}{K_{AOB,\,NO}+S_{NO}}\times X_{AOB}$
NO reduction to N_2O by AOB	$\eta_{AOB}\times\mu_{AOB,\,HAO,\,1}\times\frac{S_{NO}}{K_{AOB,\,NO}+S_{NO}}\times\frac{S_{NH2OH}}{K_{AOB,\,NH2OH}+S_{NH2OH}}\times X_{AOB}$
Decay of AOB	$b_{AOB}\times X_{AOB}$
Growth of NOB	$\mu_{NOB}\times\frac{S_{O2}}{K_{NOB,\,O2}+S_{O2}}\times\frac{S_{NO2}}{K_{NOB,\,NO2}+S_{NO2}}\times X_{NOB}$
Decay of NOB	$b_{NOB}\times X_{NOB}$
Hydrolysis	$k_H\times\frac{\frac{X_S}{X_{HB}}}{K_X+\frac{X_S}{X_{HB}}}\times\left[\frac{S_{O2}}{K_{HB,\,O2,\,1}+S_{O2}}+\eta_h\times\left(\frac{K_{HB,\,O2,\,1}}{K_{HB,\,O2,\,1}+S_{O2}}\times\frac{S_{NO3}+S_{NO2}+S_{NO}+S_{N2O}}{K_{HB,\,NO3}+S_{NO3}+S_{NO2}+S_{NO}+S_{N2O}}\right)\right]\times X_{HB}$
Aerobic growth of HB	$\mu_{HB}\times\frac{S_{O2}}{K_{HB,\,O2,\,1}+S_{O2}}\times\frac{S_S}{K_{HB,\,S,\,1}+S_S}\times X_{HB}$
Anoxic growth of HB on nitrate	$\eta_{HB,\,1}\times\mu_{HB}\times\frac{K_{HB,\,O2,\,2}}{K_{HB,\,O2,\,2}+S_{O2}}\times\frac{S_{NO3}}{K_{HB,\,NO3}+S_{NO3}}\times\frac{S_S}{K_{HB,\,S,\,2}+S_S}\times X_{HB}$
Anoxic growth of HB on nitrite	$\eta_{HB,\,2}\times\mu_{HB}\times\frac{K_{HB,\,O2,\,3}}{K_{HB,\,O2,\,3}+S_{O2}}\times\frac{S_{NO2}}{K_{HB,\,NO2}+S_{NO2}}\times\frac{S_S}{K_{HB,\,S,\,3}+S_S}\times\frac{K_{HB,\,NO,\,I1}}{K_{HB,\,NO,\,I1}+S_{NO}}\times X_{HB}$
Anoxic growth of HB on NO	$\eta_{HB,\,3}\times\mu_{HB}\times\frac{K_{HB,\,O2,\,4}}{K_{HB,\,O2,\,4}+S_{O2}}\times\frac{S_{NO}}{K_{HB,\,NO}+S_{NO}+\frac{(S_{NO})^2}{K_{HB,\,NO,\,I2}}}\times\frac{S_S}{K_{HB,\,S,\,4}+S_S}\times X_{HB}$
Anoxic growth of HB on N_2O	$\eta_{HB,\,4}\times\mu_{HB}\times\frac{K_{HB,\,O2,\,5}}{K_{HB,\,O2,\,5}+S_{O2}}\times\frac{S_{N2O}}{K_{HB,\,N2O}+S_{N2O}}\times\frac{S_S}{K_{HB,\,S,\,5}+S_S}\times\frac{K_{HB,\,NO,\,I3}}{K_{HB,\,NO,\,I3}+S_{NO}}\times X_{HB}$
Decay of HB	$b_{HB}\times X_{HB}$

Table S4. Values of key parameters for the simulation

Parameter	Definition	Unit	Value	Reference
AOB				
$\mu_{AOB,\,AMO}$	Maximum specific growth rate of AOB for ammonium oxidation to NH_2OH	1/h	0.205	[1]
$\mu_{AOB,\,HAO,\,1}$	Maximum specific growth rate of AOB for NH_2OH oxidation to NO or NO reduction to N_2O	1/h	0.085	[1]
$\mu_{AOB,\,HAO,\,2}$	Maximum specific growth rate of AOB for NO oxidation to N_2O	1/h	0.567	[1]
b_{AOB}	Decay rate coefficient of AOB	1/h	0.0054	[2]
$K_{AOB,\,O2,\,1}$	Half saturation constant of AOB for oxygen	g DO/m^3	0.4	[1]
$K_{AOB,\,O2,\,2}$	Half saturation constant of AOB for oxygen	g DO/m^3	0.073	[1]
$K_{AOB,\,NH4}$	Half saturation constant of AOB for ammonia	g N/m^3	2.4	[1]
$K_{AOB,\,NH2OH}$	Half saturation constant of AOB for hydroxylamine	g N/m^3	2.4	[1]
$K_{AOB,\,NO}$	Half saturation constant of AOB for nitric oxide	g N/m^3	0.0084	[1]
η_{AOB}	Reduction factor	-	0.285	[1]

Table S4. Continued

NOB				
μ_{NOB}	Maximum specific growth rate of NOB	1/h	0.06	[3]
b_{NOB}	Decay rate coefficient of NOB	1/h	0.0025	[3]
$K_{NOB, NO2}$	Half saturation constant of NOB for oxygen	g DO/m^3	2.2	[3]
$K_{NOB, NO2}$	Half saturation constant of NOB for nitrite	g N/m^3	5.5	[3]
HB				
μ_{HB}	Maximum specific growth rate of HB	1/h	0.26	[4]
$\eta_{HB,1}$	Reduction factor for HB growth	-	0.28	[4]
$\eta_{HB,2}$	Reduction factor for HB growth	-	0.16	[4]
$\eta_{HB,3}$	Reduction factor for HB growth	-	0.35	[4]
$\eta_{HB,4}$	Reduction factor for HB growth	-	0.35	[4]
b_{HB}	Decay rate coefficient of HB	1/h	0.017	[4]
$K_{HB, O2, 1}$	Half saturation constant of HB for oxygen	g DO/m^3	0.1	[4]
$K_{HB, O2, 2}$	Half saturation constant of HB for oxygen	g DO/m^3	0.1	[4]
$K_{HB, O2, 3}$	Half saturation constant of HB for oxygen	g DO/m^3	0.1	[4]
$K_{HB, O2, 4}$	Half saturation constant of HB for oxygen	g DO/m^3	0.1	[4]
$K_{HB, O2, 5}$	Half saturation constant of HB for oxygen	g DO/m^3	0.1	[4]
$K_{HB, S, 1}$	Half saturation constant of HB for soluble organics	gCOD/m^3	20	[4]
$K_{HB, S, 2}$	Half saturation constant of HB for soluble organics	gCOD/m^3	20	[4]
$K_{HB, S, 3}$	Half saturation constant of HB for soluble organics	gCOD/m^3	20	[4]
$K_{HB, S, 4}$	Half saturation constant of HB for soluble organics	gCOD/m^3	20	[4]
$K_{HB,S,5}$	Half saturation constant of HB for soluble organics	gCOD/m^3	40	[4]
$K_{HB, NO3}$	Half saturation constant of HB for nitrate	g N/m^3	0.2	[4]
$K_{HB, NO2}$	Half saturation constant of HB for nitrite	g N/m^3	0.2	[4]
$K_{HB, NO}$	Half saturation constant of HB for nitric oxide	g N/m^3	0.05	[4]
$K_{HB, N2O}$	Half saturation constant of HB for nitrous oxide	g N/m^3	0.05	[4]
$K_{HB, NO, I1}$	Inhibitory coefficient of NO	g N/m^3	0.5	[4]
$K_{HB, NO, I2}$	Inhibitory coefficient of NO	g N/m^3	0.3	[4]
$K_{HB, NO, I3}$	Inhibitory coefficient of NO	g N/m^3	0.075	[4]
η_Y	Anoxic yield factor	-	0.9	[4]
η_h	Reduction factor for anaerobic X_{HB} growth	-	0.4	[4]
k_h	Hydrolysis rate constant	1/h	0.125	[5]
K_X	Hydrolysis saturation constant	g COD/g COD	1.0	[5]
Stoichiometric parameters				
Y_{AOB}	Yield coefficient for X_{AOB}	g COD/g N	0.15	[6]
Y_{NOB}	Yield coefficient for X_{NOB}	g COD/g N	0.041	[3]
Y_{HB}	Yield coefficient for X_{HB}	g COD/g COD	0.6	[4]
i_{NXB}	Nitrogen content in biomass	g N/g COD	0.07	[5]
i_{NXI}	Nitrogen content in X_I	g N/g COD	0.02	[5]
f_I	X_I fraction in biomass decay	g COD/g COD	0.1	[5]
Mass transfer coefficients				
D_{NH4}	Diffusion coefficient of NH_4^+ in water	m^2/d	1.5×10^{-4}	[7]
D_{NO2}	Diffusion coefficient of NO_2^- in water	m^2/d	1.4×10^{-4}	[7]
D_{NO3}	Diffusion coefficient of NO_3^- in water	m^2/d	1.4×10^{-4}	[7]
D_S	Diffusion coefficient of COD in water	m^2/d	1.0×10^{-4}	[8]
D_{N2}	Diffusion coefficient of N_2 in water	m^2/d	1.73×10^{-4}	[9]
D_{O2}	Diffusion coefficient of O_2 in water	m^2/d	1.99×10^{-4}	[9]
D_{NH2OH}	Diffusion coefficient of hydroxylamine in water	m^2/d	1.03×10^{-6}	[10]
D_{NO}	Diffusion coefficient of nitric oxide in water	m^2/d	7.52×10^{-6}	[11]
D_{N2O}	Diffusion coefficient of nitrous oxide in water	m^2/d	1.82×10^{-4}	[12]

Table S4. Continued

Biofilm				
L_F	Biofilm thickness	m	2.0×10^{-4}	This study
			4.0×10^{-4}	
			6.0×10^{-4}	
			8.0×10^{-4}	
			1.0×10^{-3}	
rho	Biofilm density	g COD/m^3	5.0×10^{5}	[13]
θ	Biofilm porosity	m^3/m^3	0.80	[14]

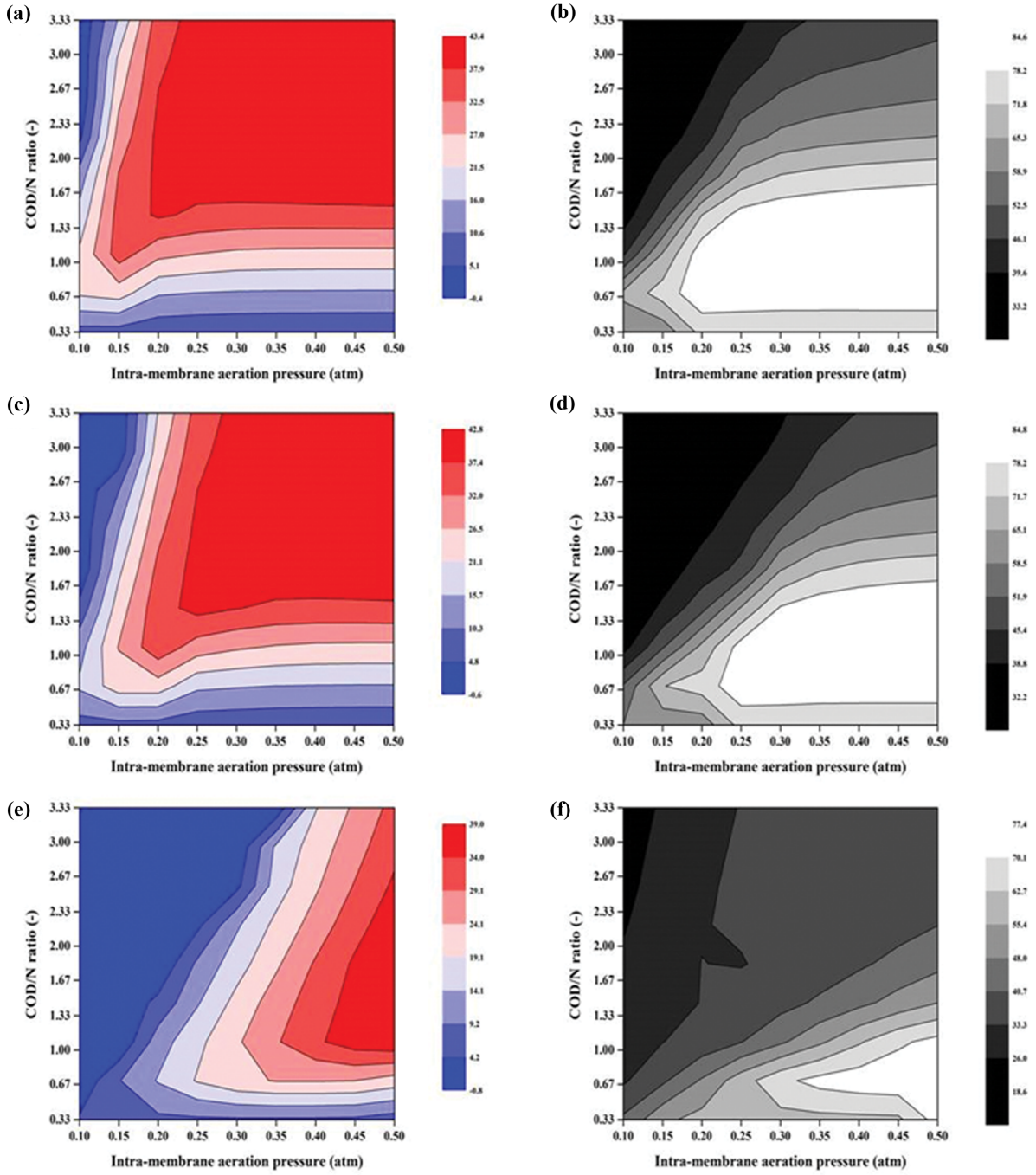


Fig. S1. Removal performance of total nitrogen and soluble organics of MAB on the membrane with different oxygen transfer coefficients: (a), (b) for 7.5 m/d, (c), (d) for 1.5 m/d and (e), (f) for 0.3 m/d.

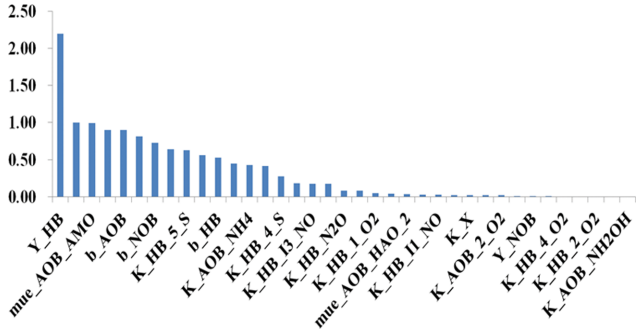


Fig. S2. Mean abs. of sensitivity function for the total nitrogen removal of MAB on the membrane with oxygen transfer coefficient of 1.5 m/d under influent COD/N ratio of 0.67 and intra-membrane aeration pressure of 0.20 atm (L_F=400 μm).

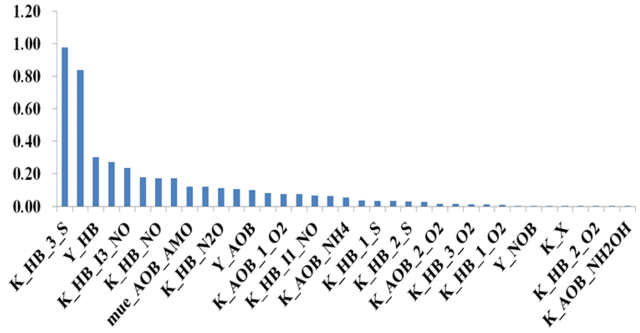


Fig. S3. Mean abs. of sensitivity function for the nitrous oxide production of MAB on the membrane with oxygen transfer coefficient of 1.5 m/d under influent COD/N ratio of 0.67 and intra-membrane aeration pressure of 0.20 atm (L_F=400 μm).

ADDITIONAL REFERENCES

1. B.-J. Ni and Z. Yuan, *Water Res.*, **87**, 336 (2015).
2. B.-J. Ni, M. Ruscalleda, C. Pellicer-Nacher and B. F. Smets, *Environ. Sci. Technol.*, **45**, 7768 (2011).
3. U. Wiesmann, *Adv. Biochem. Eng. Biot.*, **51**, 113 (1994).
4. W. C. Hiatt and C. P. L. Grady, *Water Environ. Res.*, **80**, 2145 (2008).
5. M. Henze, W. Gujer, T. Mino and M. C. M. van Loosdrecht, *Activated sludge models ASM1, ASM2, ASM2d and ASM3*, IWA Scientific Technical Report 9, London: IWA Publishing (2000).
6. B.-J. Ni, Z. Yuan and K. Chandran, *Biotechnol. Bioeng.*, **110**, 153 (2013).
7. K. Williamson and P. L. McCarty, *Journal (Water Pollution Control Federation)*, **48**, 281 (1976).
8. X. D. Hao and M. C. M. van Loosdrecht, *Water Sci. Technol.*, **49**, 83 (2004).
9. P. T. H. M. Verhallen, L. J. P. Oomen, A. J. J. M. v. d. Elsen, J. Kruger and J. M. H. Fortuin, *Chem. Eng. Sci.*, **39**, 1535 (1984).
10. H. R. Zare and N. Nasirizadeh, *Electroanal.*, **18**, 507 (2006).
11. J. M. Vanderkooi, W. W. Wright and M. Erecinska, *Biochimica et Biophysica Acta (BBA)-Protein Structure and Molecular Enzymology*, **1207**, 249 (1994).
12. W. M. Henes, *CRC handbook of chemistry and physics*, 97th Ed., CRC Press, Taylor & Francis Group, Boca Raton (2016).
13. G. Koch, K. Egli, J. R. van der Meer and H. Siegrist, *Water Sci. Technol.*, **41**, 191 (2000).
14. R. Reichert, *AQUASIM 2.0d user manual, Computer program for the identification and simulation of aquatic systems*, Swiss Federal Institute for Environmental Science and Technology (EAWAG), Dubendorf, Switerland (1998).